

NAVY PHASE I SBIR FINAL REPORT

**Contract Monitor:**           **Dr. Deborah Van Vechten**  
   **Office of Naval Research**  
   **800 N. Quincy Street**  
   **Arlington, VA 22217**

**Contract Title:**               ***“Ultra-Low Heat Leak YBCO Superconducting Leads for Cryoelectronic Applications”***

**Contract Number:**           **N00014-04-M-0116**

**Reporting Period:**           **May 1st, 2004 – December 31st, 2004**

**Principal Investigator:**     **Robert Webber**  
   **HYPRES, Inc.**  
   175 Clearbrook Road  
   **Elmsford, NY 10523**  
   PHONE       (914) 592-1190 x7826  
   FAX         (914) 347-2239  
   E-MAIL      [webber@hypres.com](mailto:webber@hypres.com)

Report Documentation Page			Form Approved OMB No. 0704-0188		
Public reporting burden for the collection of information is estimated to average 1 hour per response, including the time for reviewing instructions, searching existing data sources, gathering and maintaining the data needed, and completing and reviewing the collection of information. Send comments regarding this burden estimate or any other aspect of this collection of information, including suggestions for reducing this burden, to Washington Headquarters Services, Directorate for Information Operations and Reports, 1215 Jefferson Davis Highway, Suite 1204, Arlington VA 22202-4302. Respondents should be aware that notwithstanding any other provision of law, no person shall be subject to a penalty for failing to comply with a collection of information if it does not display a currently valid OMB control number.					
1. REPORT DATE <b>31 DEC 2004</b>		2. REPORT TYPE <b>N/A</b>		3. DATES COVERED <b>-</b>	
4. TITLE AND SUBTITLE <b>Ultra-Low Heat Leak YBCO Superconducting Leads for Cryoelectronic Applications</b>				5a. CONTRACT NUMBER <b>N00014-04-M-0116</b>	
				5b. GRANT NUMBER	
				5c. PROGRAM ELEMENT NUMBER	
6. AUTHOR(S)				5d. PROJECT NUMBER	
				5e. TASK NUMBER	
				5f. WORK UNIT NUMBER	
7. PERFORMING ORGANIZATION NAME(S) AND ADDRESS(ES) <b>Hypres, Inc., 175 Clearbrook Road, Elmsford, NY 10523</b>				8. PERFORMING ORGANIZATION REPORT NUMBER	
9. SPONSORING/MONITORING AGENCY NAME(S) AND ADDRESS(ES)				10. SPONSOR/MONITOR'S ACRONYM(S)	
				11. SPONSOR/MONITOR'S REPORT NUMBER(S)	
12. DISTRIBUTION/AVAILABILITY STATEMENT <b>Approved for public release, distribution unlimited</b>					
13. SUPPLEMENTARY NOTES <b>The original document contains color images.</b>					
14. ABSTRACT					
15. SUBJECT TERMS					
16. SECURITY CLASSIFICATION OF:			17. LIMITATION OF ABSTRACT <b>UU</b>	18. NUMBER OF PAGES <b>13</b>	19a. NAME OF RESPONSIBLE PERSON
a. REPORT <b>unclassified</b>	b. ABSTRACT <b>unclassified</b>	c. THIS PAGE <b>unclassified</b>			

## CONTENTS

Introduction.....	2
1.0 Thick-Film YBCO Lead Development.....	2
1.1 BaZrO <sub>3</sub> buffer layer formed via YSZ reaction with liquid BaO <sub>2</sub> .....	2
1.2 BaZrO <sub>3</sub> buffer layer formed via Sol-Gel Reaction at Lower Temperature .....	4
1.3 YBa <sub>2</sub> Cu <sub>3</sub> O <sub>7</sub> superconducting leads .....	4
2.0 Thermal Conductivity Measurements.....	8
2.1 Thermal Conductivity of polycrystalline yttria stabilized zirconia substrates....	8
2.2 Thermal Conductivity of Nickel-5% Tungsten Substrates .....	11
Conclusion .....	12
APPENDIX A.....	13

## Introduction

Recent developments in fuel-cell research have led to the availability of commercially manufactured flexible polycrystalline sheets of yttria stabilized zirconia (YSZ) in thicknesses of 50 to 100  $\mu\text{m}$ , which are ideal substrates for laying down low-current DC leads of YBa<sub>2</sub>Cu<sub>3</sub>O<sub>7- $\delta$</sub>  (YBCO) that conduct very little heat at cryogenic temperatures. Production of thick films of YBCO (several tens of microns thick), albeit at lower current densities than thin films (approx. 1 $\mu\text{m}$ ), was well established by the mid-nineties using relatively simple “low-tech” methods.

As was shown in the phase I proposal, the combination of these two materials can, in theory, create a superconducting DC lead which achieves our target for specific heat load (heat-load per unit amp for 35mA current passing between a 60K and a 4K heat station), i.e. 1mW per amp of current delivered. *See appendix A.* Calculations also showed that the same materials could also produce higher performance coplanar waveguides than normal metals at a range of RF frequencies.

A key problem to be solved in producing thick-film YBCO on YSZ is that the YBCO must be sintered at a high temperature on top of the substrate. This allows the chemical interaction between them, since Zr<sup>4+</sup> can dope the YBCO, lowering J<sub>c</sub>, and Ba<sup>2+</sup> can react with the ZrO<sub>2</sub>, altering the local stoichiometry of the YBCO. A separate *diffusion barrier* is needed to prevent this from happening, and most of the materials science work carried out by our subcontractor (Industrial Research Limited), was devoted towards developing this barrier layer.

At Hypres, a method for measuring the thermal conductivities of materials used in these composite leads, as a function of temperature, was developed. Such measurements of low thermal conductivity materials need to be made in an insulating vacuum (to reduce parasitic thermal effects) and a two-stage cryocooler provided stable temperature stations.

## 1.0 Thick-Film YBCO Lead Development

### 1.1 BaZrO<sub>3</sub> buffer layer formed via YSZ reaction with liquid BaO<sub>2</sub>

Buffer layers of BaZrO<sub>3</sub> were formed on YSZ substrates using the reaction between a melt of BaO<sub>2</sub>, maintained at 1050 °C under 40 kBar O<sub>2</sub>, and the Zr(Y)O<sub>2</sub> substrate. Allowing the reaction to proceed for 0.5 to 2 hours gave rise to layers 5 to 20  $\mu\text{m}$  in thickness. The chemical

composition of the layers, deduced from EDS analysis on cross-sections, suggested that the layers were a mixture of  $\text{BaZrO}_3$  and  $\text{BaO}$ , with a stoichiometry of approximately  $\text{Ba}_2\text{ZrO}_4$ . This observation was confirmed by x-ray diffraction measurements from the surface. In addition the layer was fragile, being easily detached from the substrate when any excess  $\text{BaO}_2$  melt material adhering to the surface was dissolved off in dilute acid, presumably as the  $\text{BaZrO}_3$  layer was disrupted.

The “melt immersion” method of producing the  $\text{BaZrO}_3$  buffer layer was abandoned because:

- a) The layer remains chemically active – any embedded  $\text{BaO}_2$  or  $\text{BaO}$  being available to modify the stoichiometry of the YBCO film subsequently laid down.
- b) Attachment to the substrate was not sufficient to ensure survival of a coherent layer through any chemical or mechanical cleaning step by which any excess  $\text{BaO}_2$  could be removed.

In the course of this process development project,  $\text{BaZrO}_3$  buffer layers have been successfully established, continuous and cohering to the substrate, only by screen-printing a thick layer of the  $\text{BaO}_2$  reactant onto the substrate. The substrate was then held in the reaction zone – temperature,  $\text{O}_2$  pressure – for sufficient time for all of the reactant to be consumed and a dense  $\text{BaZrO}_3$  layer generated. There are difficulties, as yet unsolved, in ensuring that the  $\text{BaO}_2$  liquid phase wetted the entire surface of the substrate. Occasionally it did happen and one of these successfully coated substrates was used to make a pair of test superconducting leads. (Section 1.3)

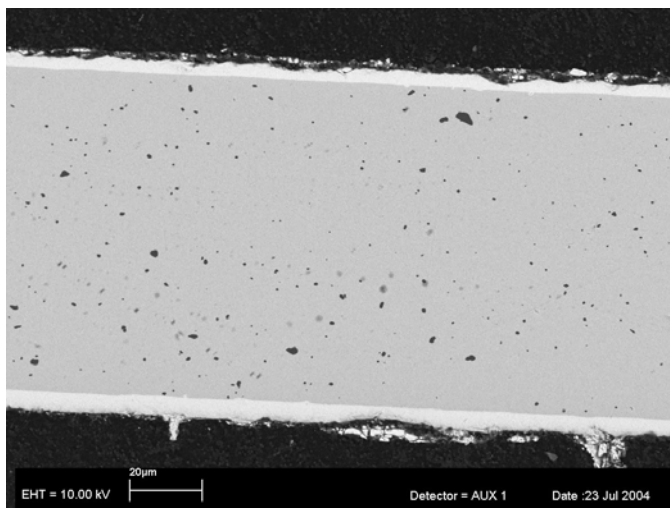


*Figure 1 Electron micrograph of section through the 100  $\mu\text{m}$  thick YSZ sheet. The dense white layers on the top and bottom are of barium zirconate, the desired buffer layer. That the surface film is  $\text{BaZrO}_3$  was confirmed using electron-dispersive x-ray energy analysis and x-ray diffraction. (The dark spots within the YSZ substrate were analyzed to be  $\text{Al}_2\text{O}_3$  – but we have no idea why these are present in the material.)*

## 1.2 BaZrO<sub>3</sub> buffer layer formed via Sol-Gel Reaction at Lower Temperature

Following the lack of repeatability of the above barium oxide melt method, IRL chose to deposit the reactants needed for formation of BaZrO<sub>3</sub> on the surface of the YSZ in a gel solution. This can be “spun” onto the surface in a thin uniform layer, and reaction of the constituents (which takes place at a much lower temperature than the melt method) also produces an even layer.

Barium trifluoroacetate and zirconium propionate can be dissolved in ethanol to form a sol gel precursor for barium zirconate. This precursor was spun onto a 10 mm square polycrystalline YSZ substrate forming a uniform layer. The green film was then reacted at ~ 600 °C, yielding a thin (~1 μm), dense, coherent film of BaZrO<sub>3</sub> (see *figure 2*). The method had been successfully tested on single-crystal substrate [Long, Kodankandath, unpublished], but this was the first time it was demonstrated on a small sample of the polycrystalline material.

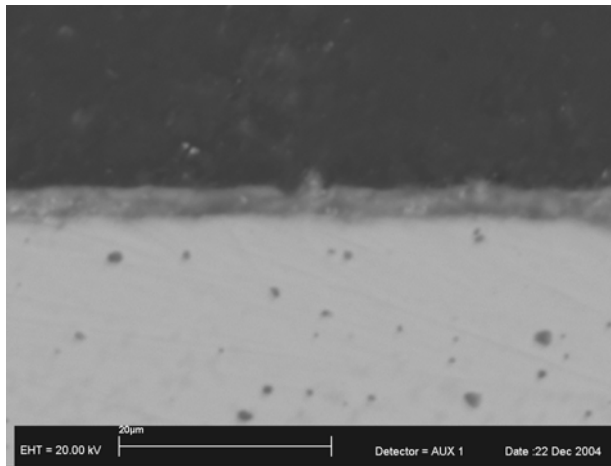


*Figure 2* Cross section of YSZ substrate with barium zirconate buffer layer approximately 1 micron thickness, formed by the sol-gel method.

Since this work was performed at the very end of phase I, no YBCO lines were deposited on the resultant buffer-layer-coated samples. However, three such samples were produced, all with apparent high quality BaZrO<sub>3</sub> layers, showing that the method was quite reproducible.

## 1.3 YBa<sub>2</sub>Cu<sub>3</sub>O<sub>7</sub> superconducting leads

A BaZrO<sub>3</sub>-coated YSZ substrate was sawn into 4 pieces – dimensions 10.2 x 1.7 x 0.1 mm each. An ink of YBa<sub>2</sub>Cu<sub>3</sub>O<sub>7</sub> powder (SCI Engineered Materials), believed to be phase pure and of average particle size less than 5 μm, was created. The powder was dispersed with 1.5% (w/w) menhaden oil (Sigma Chemical Co.) in dry isopropanol using high-speed shear-mixing. The solvent was evaporated off at ~ 60 °C and the powder then thoroughly mixed with ~ 60% (v/v) α-terpineol (Aldrich Chemical Co.). More terpineol was slowly added, with mixing, until the ink acquired a suitable viscosity for screen-printing. The thick film, covering the whole surface, was printed onto the buffered substrates through a 120-mesh screen – which can be expected to deposit 75 μm “mesas” spreading to a continuous film ~ 35 μm in thickness. The leads were thermally treated, in a continuous process:

1. Evaporate organic components off at 200 °C under nitrogen;
2. Burn out remnant organic components at 400 °C under oxygen;

3. Sinter the  $\text{YBa}_2\text{Cu}_3\text{O}_7$  under 1 bar oxygen at 965 °C – the temperature at which there is an equilibrium amongst  $\text{YBa}_2\text{Cu}_3\text{O}_7$ ,  $\text{Y}_2\text{BaCuO}_5$  and a liquid ( $\text{BaCuO}_2$ ) phase; then
4. Slow cool to below 400 °C, allowing the  $\text{YBa}_2\text{Cu}_3\text{O}_7$  to fully oxygen load. Then
5. Silver contact electrodes were painted across the ends of the leads and sintered at 500 °C, before again allowing to slow cool in 1 bar oxygen.

Silver wire leads were attached to the contact pads with In-solder and the lead unit mounted beneath spring-loaded contacts, 5 mm apart, which were then pressed into contact with the superconducting strips. The whole device was then immersed into liquid  $\text{N}_2$  at 77 K. V-I data was obtained using a Yokogawa 7651 DC source, for setting the current, and an HP 34401 dvm to measure the voltage developed in the superconducting strip. The resulting V-I curves for two leads are displayed in *fig 3*, below.

Using the usually applied voltage criterion for the onset of superconductivity - 1 microvolt/cm - the two leads have critical currents, at 77K, of 1.7 mA and 0.13 mA only. In the low current plot for each lead, the best fit curve for  $V \sim I^n$  is displayed. This is an empirical equation from which  $n$  is commonly used to characterize the transition from superconducting to normal conduction. Commonly for sintered materials  $n \sim 10$ -14 and for thin films  $n \sim 20$ -40. Values as low as 2.9 and 1.9, as observed here, are thus extremely low and indicate that the YBCO is very poorly linked.

Scanning electron micrographs of cross sections of the leads confirm that the  $\text{YBa}_2\text{Cu}_3\text{O}_7$  strips are not well sintered (See *figure 4*).

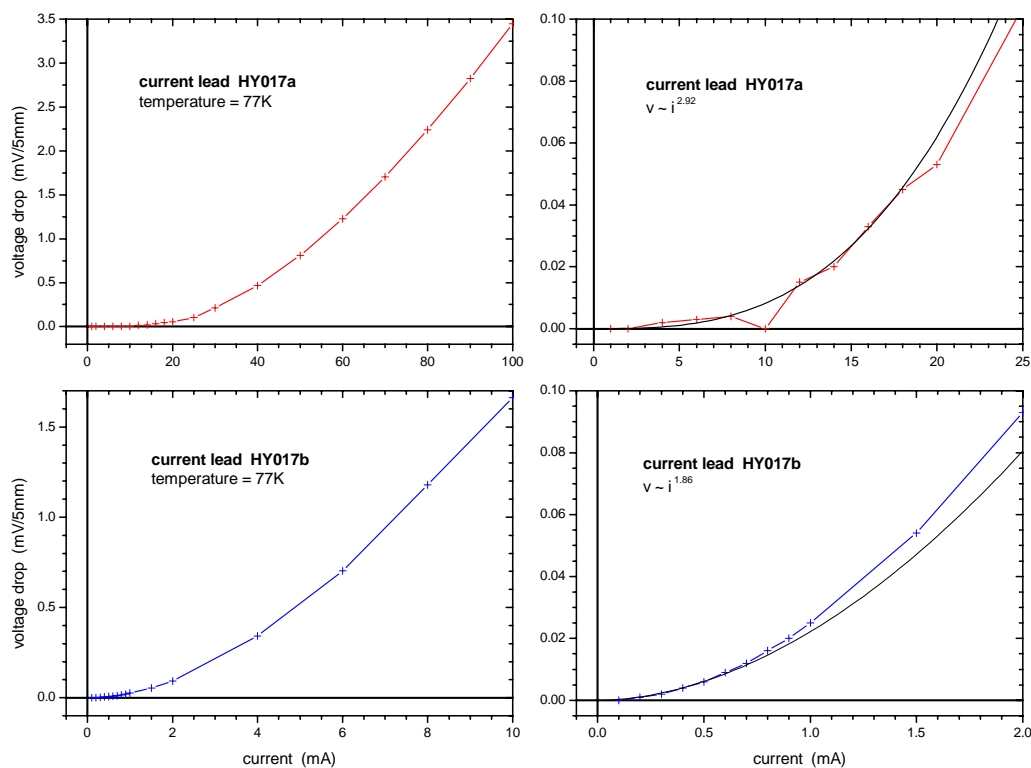


Figure 3: V-I data for two  $\text{YBa}_2\text{Cu}_3\text{O}_7$  strips laid on  $\text{BaZrO}_3$  buffered YSZ substrates.

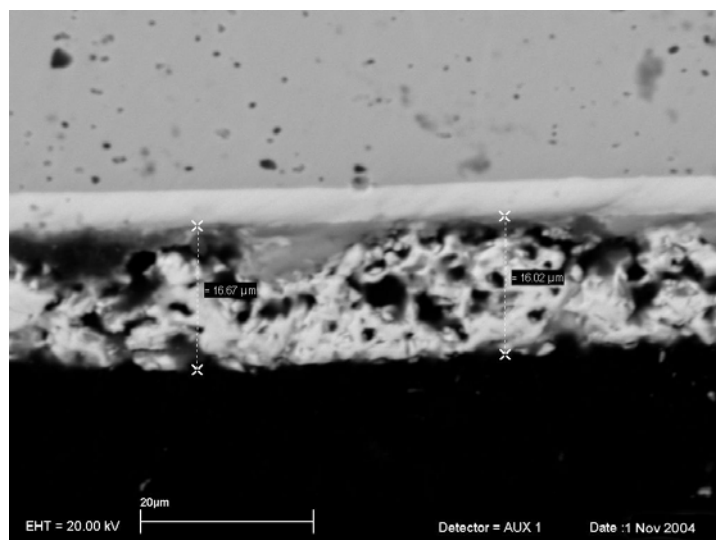


Figure 4: Cross-section of current lead. The YSZ substrate lies at the top of the micrograph – and contains particulate  $\text{Al}_2\text{O}_3$  (the dark spots). A dense layer of  $\text{BaZrO}_3$ ,  $\sim 4 \mu\text{m}$  thick has been formed at the substrate surface; and a porous layer of  $\text{YBa}_2\text{Cu}_3\text{O}_7$ ,  $16 \mu\text{m}$  thick, has been sintered on the surface of the  $\text{BaZrO}_3$ .

Composition of the components was determined by energy dispersive x-ray spectroscopy, which also showed that a small amount of Cu was detectable in the BaZrO<sub>3</sub> layer, concentrated toward the interface with the YBa<sub>2</sub>Cu<sub>3</sub>O<sub>7</sub> layer. However this observation must be interpreted carefully since the volume of material, from around the incident point of the e-beam, that is analyzed is ~ 1 μm diameter. There has been no detachment of the buffer or superconducting layers from the substrate despite two cycles of temperature between 500 °C and room temperature, and several cycles of temperature between 77 K and room temperature. Differential thermal expansion of the layers appears to be minimal.

It is clear that the sintering conditions for the YBa<sub>2</sub>Cu<sub>3</sub>O<sub>7</sub> were not ideal, and maybe that some of the highly fluid BaCuO<sub>2</sub> melt has penetrated the BaZrO<sub>3</sub> layer, reacting with it. Such a process would disturb the stoichiometry of the YBa<sub>2</sub>Cu<sub>3</sub>O<sub>7</sub> layer, leading to poor connectivity between the superconducting grains. Further exploration of the sintering conditions for the YBa<sub>2</sub>Cu<sub>3</sub>O<sub>7</sub> – temperature, oxygen pressure and time – are necessary to optimize the critical current density in the thick film. The current densities achieved in the present films were only ~ 6 A cm<sup>-2</sup> and 0.5 A cm<sup>-2</sup> respectively – considerably less than the values of ~ 1200 A cm<sup>-2</sup> which can be achieved in sintered pellets (the goal for current leads in the first part of this development program was 800 A cm<sup>-2</sup>).

In order to produce practical low-conductivity current leads using patterned YBa<sub>2</sub>Cu<sub>3</sub>O<sub>7</sub> thick film conductors, considerable development work is required to sinter a dense layer of YBa<sub>2</sub>Cu<sub>3</sub>O<sub>7</sub> onto the buffer layer, controlling the formation of the partial melt so that little BaCuO<sub>2</sub> is sequestered into the buffer layer and full recrystallization of well-connected grains of YBa<sub>2</sub>Cu<sub>3</sub>O<sub>7</sub> takes place:

The present series of trials, and work reported in the research literature, suggest that this can be achieved.



## 2.0 Thermal Conductivity Measurements

Critical to the performance of the composite YBCO leads, is knowledge of the thermal conductivity as a function of temperature of its various components. The thermal conductivity of such samples has been measured using the apparatus depicted in *figure 5*. By applying a series of different values of heater power to the floating end of the sample and measuring the temperature difference between the two ends when in thermal equilibrium, the thermal conductivity integral and hence the thermal conductivity as a function of temperature can be measured.

For heat conduction along a material of uniform cross-sectional area  $A$ , length  $L$ , thermal conductivity  $k(T)$  where  $T$  is temperature and  $T_0$  and  $T_1$  are the temperatures of the cold and warm end respectively, then,  $\dot{Q}$ , the rate of heat conducted through the material is given by:

$$\dot{Q} = \frac{A}{L} \int_{T_0}^{T_1} k dT \quad \text{Equ. 1}$$

If two different heat loads  $\dot{Q}_j$  and  $\dot{Q}_{j+1}$  are applied, and corresponding end temperatures are measured, then the thermal conductivity at the mean of these two temperatures is given by:

$$k_{\frac{(T_{j+1}+T_j)}{2}} = \frac{L}{A} \left( \frac{\dot{Q}_{j+1} - \dot{Q}_j}{T_{j+1} - T_j} \right) \quad \text{Equ. 2}$$

### 2.1 Thermal Conductivity of polycrystalline yttria stabilized zirconia substrates

Figure 7 shows the directly measured thermal conductivity integral of the sample. By changing the effective cross-sectional area and length of the sample, and performing two separate measurements, the parasitic effects were taken into account; this allows extrapolation to zero sample cross-section at which point, only parasitic heat flow remains.

Figure 8 shows the thermal conductivity derived by differentiating the integral of figure 7. The effects of the parasitic loads are also shown (the “*without parasitic*” curve is our best estimate of the true thermal conductivity). Note that these results appear to be consistent with Harshavardhan’s results at 77K. This result was used in the calculation of appendix A.

By the end of phase one, no suitable samples of substrates coated with the barium zirconate buffer layer or YBCO were available for measurement.

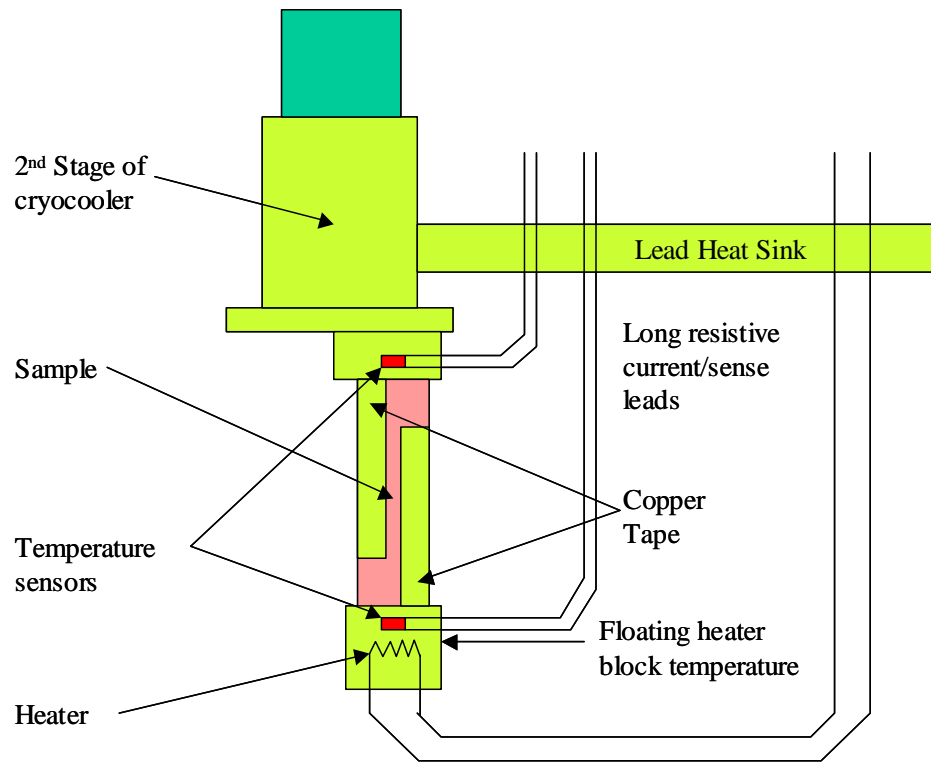


Figure 5: Schematic drawing of method for thermal conductivity measurements. The heater end of the sample is thermally “floating” and it is hoped that all the heat that is applied to it through the heater is conducted through the sample; in practice, there will be other parasitic paths for heat to flow e.g. instrumentation leads; there will also be sources of heat other than the heater e.g. black-body radiation.

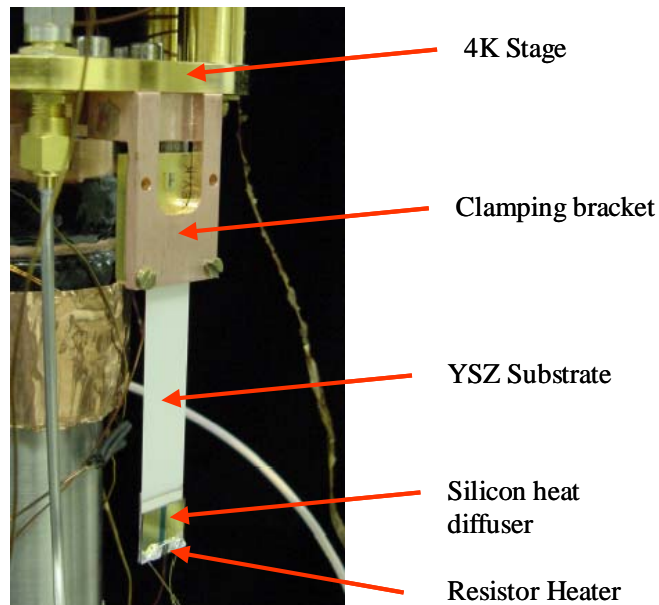


Figure 6: Photograph showing apparatus with YSZ substrate as the sample to be measured.

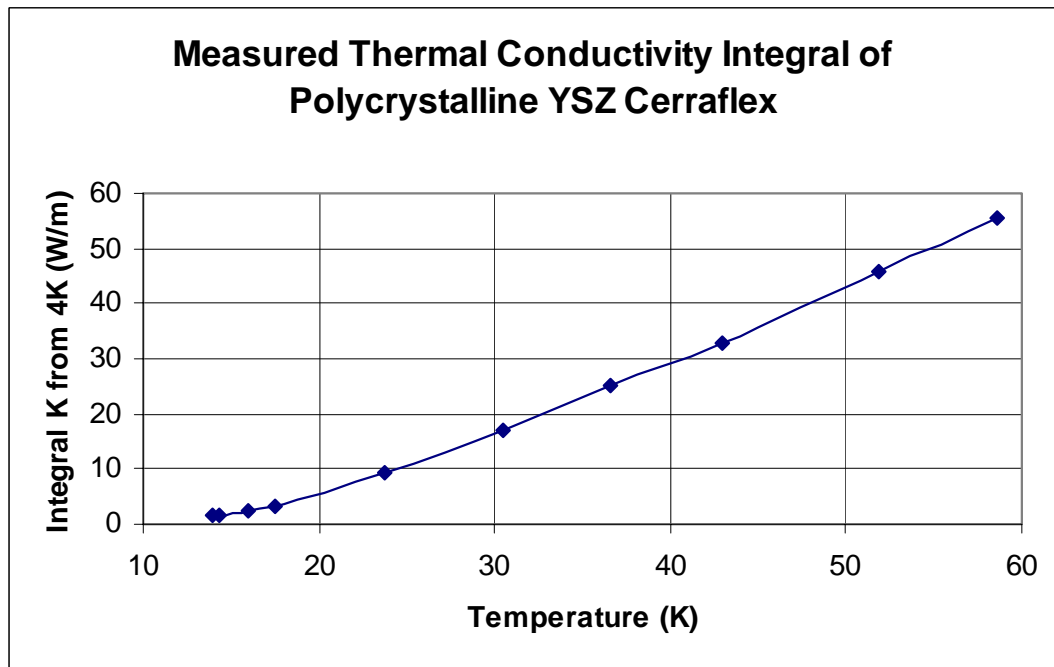


Figure 7: Directly measured thermal conductivity integral of polycrystalline yttria stabilized zirconia sample.

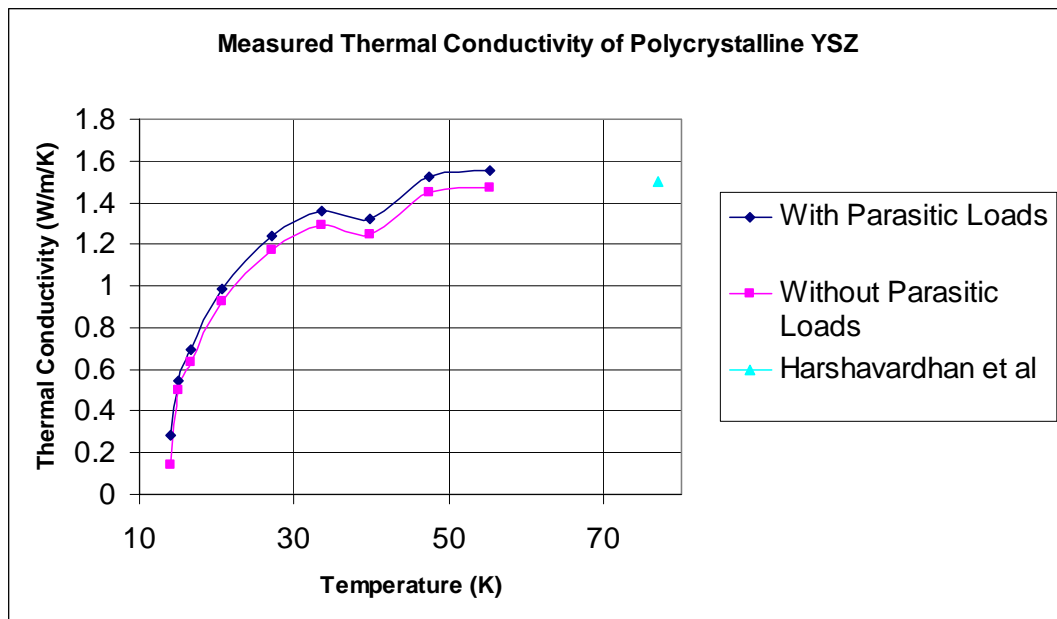


Figure 8: Thermal conductivity of YSZ sample derived by differentiation of the curve in figure 7. One data point from the literature is also included at 77K and would appear to be consistent with these measurements.

## 2.2 Thermal Conductivity of Nickel-5% Tungsten Substrates

One of the substrates proposed for use by the Tai-Yang Research Company in their phase 1 work on the same subject, is the alloy nickel-5% tungsten. A sample of this was sent to Hypres for thermal characterization. It is a 75  $\mu\text{m}$ -thick length of conductor, 1cm wide by 5cm in length, which has been cut by EDM to form a 40cm-long, 0.5mm wide strip in a concertina pattern as shown in *fig. 9*. If this sample had been set up to measure heat flow along the 40cm length, its conductance would be so small that parasitic heat loads would cause the floating end temperature to be too high, even without applying any additional heat. The relative magnitude of these parasitic effects is reduced by increasing the conductance of the sample to be measured. This was achieved by measuring heat flow across the width and not the length. Heat was injected into and extracted from the sides of the sample by suitably applied highly conductive copper tape.

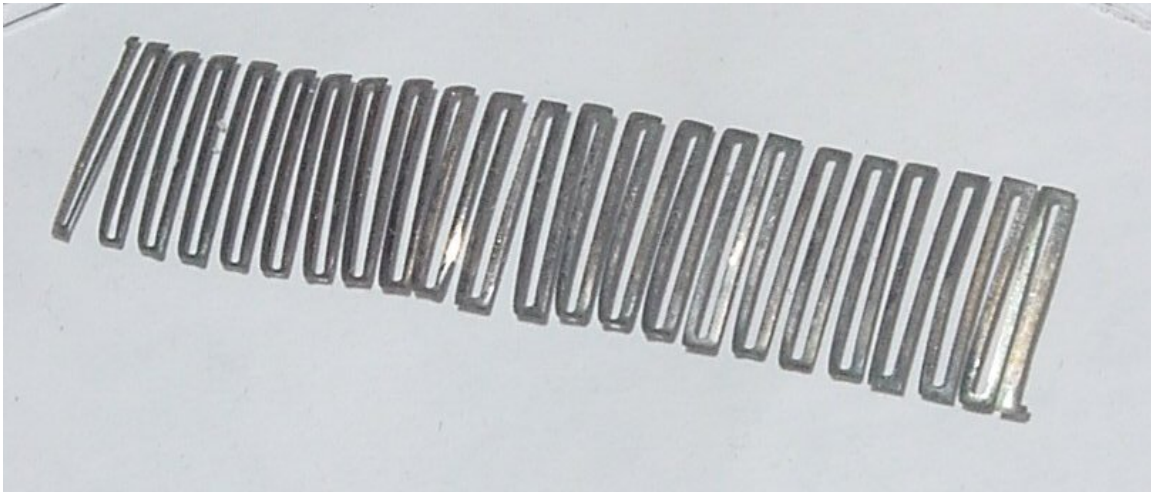


Figure 9: HTS current lead on Ni-%5W substrate (RABiTS-type) with 0.5 mm “leg” widths produced using EDM.

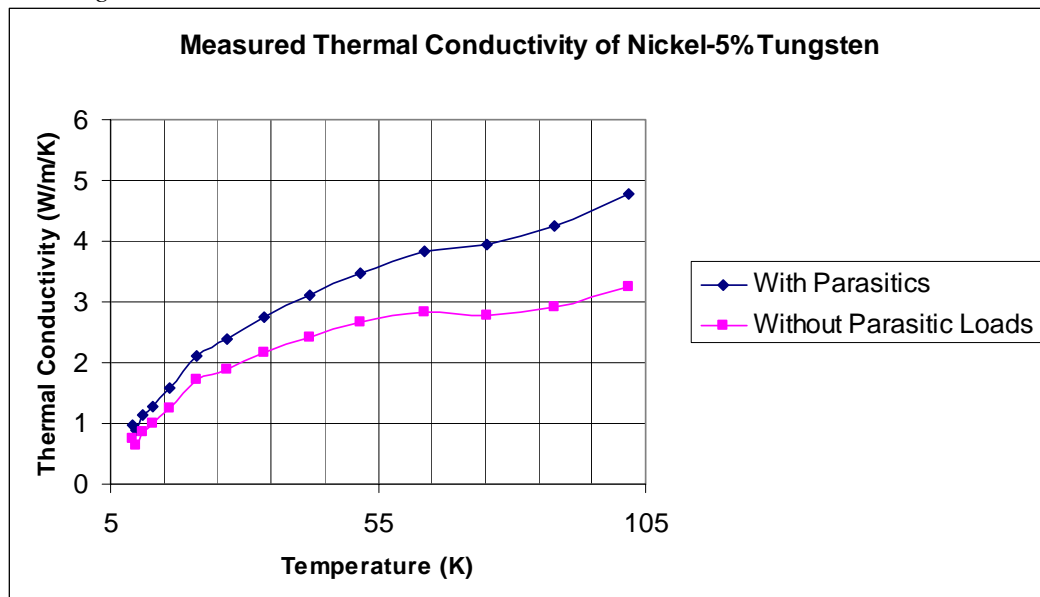


Figure 10: Measured thermal conductivity of Nickel-5% Tungsten substrate.

The magnitude of the values shown in *figure 10* is surprisingly small, and, in fact, is roughly half that of stainless steel in this temperature regime (one would not expect this material to have a thermal conductivity *lower* than the highly alloyed stainless steel). This needs to be studied in more depth, but a possible explanation is that there are additional thermal resistances in series with the sample, which are not being taken into account. The thermometers were not attached directly to the sample surface due to its size and fragility, so it is possible that they were measuring the temperature difference across the copper to sample interface also.

Further measurements should include electrical conductivity measurements as a crosscheck via the Wiedemann-Franz rule.

## Conclusion

Dense, even layers of inert barium zirconate have been deposited on polycrystalline yttria stabilized zirconia substrates as buffer layers which can allow the sintering of YBCO without its chemical reaction with the substrate. Although poorly sintered, a thick film of YBCO was formed on the top of this buffer layer, successfully demonstrating supercurrents of a few mA, albeit at extremely low current densities.

Using a barium oxide melt method, the formation of the buffer layers was difficult to control, but by applying the reactants of barium zirconate to the YSZ surface in the form of a gelatinous solution, consistently uniform dense layers were formed. They appear to be ideal to support the high temperature sintering reaction for formation of YBCO.

We have made thermal conduction measurements on 2 substrates, which are candidates for the YBCO leads. The results for YSZ are consistent with the limited data available in the literature and confirm that it is an ideal substrate material for this application.

The measured thermal conductivity values for the other substrate, nickel-5%tungsten (not a candidate for this particular thick-film application), also indicate that it is a promising substrate. Given that the apparent values are, surprisingly, significantly lower than those of stainless steel, further measurements are needed to confirm this, in the absence of any such data in the literature.

## APPENDIX A

### Predicted performance of Thick-Film YBCO and Polycrystalline YSZ Substrate

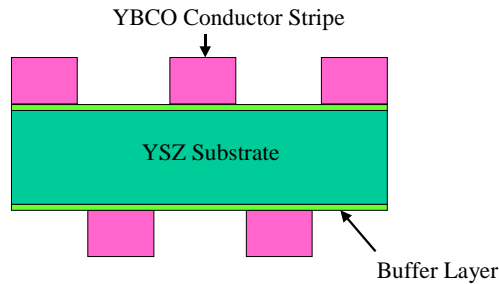


Fig. 1 Showing a cell of 5 conductor stripes in a 2-sided configuration. Each stripe is designed to operate up to a current of 100mA ( $I_c = 200\text{mA}$ ). The expected route mean square operating current per stripe is 35mA.

#### Material properties:

<b>YBa<sub>2</sub>Cu<sub>3</sub>O<sub>7</sub></b>	$\kappa = 0.4 \text{ W m}^{-1} \text{ K}^{-1}$	(4-60 K)	(ref 2 ) <sup>1</sup>
	$J_c = 800 \text{ A cm}^{-2}$	(77K)	(ref 5) <sup>2</sup>
<b>YSZ</b>	$\kappa = 1.5 \text{ W m}^{-1} \text{ K}^{-1}$	(77 K)	(ref 3) <sup>3</sup>

#### Expected performance of 5-line cell:

##### YBa<sub>2</sub>Cu<sub>3</sub>O<sub>7</sub> leads

Dimensions per line	= 75 mm x 0.5 mm x 50 $\mu\text{m}$
Heat conduction per line	= 8 $\mu\text{W}$
<b>Ic/lead</b>	= <b>0.2 A</b>

##### YSZ substrate

Dimensions	= 75 mm x 2.5 mm x 50 $\mu\text{m}$
Heat conduction	= 140 $\mu\text{W}$
<b>Total heat conduction per cell</b>	= <b>180 <math>\mu\text{W}</math></b>

**For operating current of 35 mA, the specific heat leak = 1029  $\mu\text{W/A}$   
OR 1mW/A**

**This is about 10-times less than optimized normal-metal conductors**

<sup>1</sup> H Heremans *et al*, Phys Rev B **37**, 1604 (1988)

<sup>2</sup> C Meggs *et al*, IEEE Trans Appl Supercond **9**, 676 (1999)

<sup>3</sup> K S Harshavardhan *et al*, Physica C **357-60**, 1368 (2001)